The Plant Cell, Vol. 29: 1373–1387, June 2017, www.plantcell.org © 2017 ASPB.

Cytokinin Signaling Activates *WUSCHEL* Expression during Axillary Meristem Initiation[OPEN]

Jin Wang,[a,b] Caihuan Tian,[a] Cui Zhang,[a] Bihai Shi,[a,b] Xiuwei Cao,[a,b] Tian-Qi Zhang,[c,d] Zhong Zhao,[e] Jia-Wei Wang,[c,f] and Yuling Jiao[a,b,1]

[a] State Key Laboratory of Plant Genomics, Institute of Genetics and Developmental Biology, Chinese Academy of Sciences, and National Center for Plant Gene Research, Beijing 100101, China
[b] University of Chinese Academy of Sciences, Beijing 100049, China
[c] National Key Laboratory of Plant Molecular Genetics, CAS Center for Excellence in Molecular Plant Sciences, Institute of Plant Physiology and Ecology, Shanghai Institutes for Biological Sciences, Shanghai 200032, China
[d] University of Chinese Academy of Sciences, Shanghai 200032, China
[e] School of Life Sciences, University of Science and Technology of China, Hefei, Anhui 230027, China
[f] ShanghaiTech University, Shanghai 200031, China

ORCID IDs: 0000-0002-4924-1716 (J.W.); 0000-0002-0794-5037 (C.T.); 0000-0002-6119-5572 (C.Z.); 0000-0001-8477-2048 (B.S.); 0000-0001-5204-0061 (X.C.); 0000-0003-0270-1794 (T.-Q.Z.); 0000-0001-8044-0409 (Z.Z.); 0000-0003-3885-6296 (J.-W.W.); 0000-0002-1189-1676 (Y.J.)

The homeodomain transcription factor WUSCHEL (WUS) defines the shoot stem cell niche, but the mechanisms underlying the establishment of *WUS* expression remain unclear. Here, we show that cytokinin signaling precedes *WUS* expression in leaf axils and activates *WUS* expression de novo in the leaf axil to promote axillary meristem initiation. Furthermore, type-B Arabidopsis response regulator proteins, which are transcriptional activators in the cytokinin signaling pathway, directly bind to the *WUS* promoter and activate its expression. Finally, we show that cytokinin activation of *WUS* in the leaf axil correlates with increased histone acetylation and methylation markers associated with transcriptional activation, supporting the fact that *WUS* expression requires a permissive epigenetic environment to restrict it to highly defined meristematic tissues. Taken together, these findings explain how cytokinin regulates axillary meristem initiation and establish a mechanistic framework for the postembryonic establishment of the shoot stem cell niche.

INTRODUCTION

Plant meristems are responsible for organogenesis, which can continue throughout the life of the plant. Shoot meristems harbor stem cells located in the central zone (CZ), and these cells have a lower cell division rate. Some daughter cells of the CZ cells replenish themselves in the CZ, and other cells that are closer to the peripheral zone form the organ primordia. The organizing center (OC) contains a small group of cells underneath the CZ and maintains the stem character of stem cells in the CZ. A key factor regulating shoot stem cell specification is the WUSCHEL (WUS) homeobox transcription factor (Laux et al., 1996; Mayer et al., 1998). *WUS* is expressed in the OC, which comprises the stem cell niche of shoot meristems, including the shoot apical meristems (SAMs), axillary meristems (AMs), floral meristems (FMs), and adventitious shoot meristems.

Although we do not know how *WUS* expression is established in each type of shoot meristem, extensive studies have shown both how WUS promotes shoot meristems and how *WUS* expression is maintained in them. WUS function requires interaction with transcriptional regulators of the HAIRY MERISTEM family (Zhou et al., 2015). WUS migrates from the OC to the CZ to activate the expression of the negative regulator *CLAVATA3* (*CLV3*), which encodes a secreted peptide (Fletcher et al., 1999; Yadav et al., 2011; Daum et al., 2014). The CLV3 peptide activates CLV1, a transmembrane receptor kinase expressed in the OC, and this kinase inhibits *WUS* expression via a yet unknown signaling cascade (Clark et al., 1997; Ogawa et al., 2008). Thus, the WUS-CLV feedback loop forms a self-correcting mechanism that maintains a stem cell pool of constant size (Brand et al., 2000; Schoof et al., 2000).

In addition, phytohormones also help maintain shoot stem cell homeostasis. A positive-feedback loop between WUS function and cytokinin provides positional cues for shoot meristem patterning (Leibfried et al., 2005; Gordon et al., 2009; Chickarmane et al., 2012), although the underlying molecular mechanism has not been fully resolved. A number of additional WUS targets have been identified (Leibfried et al., 2005; Busch et al., 2010; Yadav et al., 2013), supporting the idea that WUS functions as a central regulator of stem cells. In contrast to the indeterminate SAM and AM, the determinate FM only transiently maintains *WUS* expression. The MADS transcription factor AGAMOUS (AG) is activated by WUS in the FM, and AG in turn terminates *WUS* expression and thus determines floral bud growth (Lenhard et al., 2001; Lohmann et al., 2001; Liu et al., 2011). However, there is a major gap in our understanding of the mechanisms that establish the initial expression of *WUS*.

[1] Address correspondence to yljiao@genetics.ac.cn.
The author responsible for distribution of materials integral to the findings presented in this article in accordance with the policy described in the Instructions for Authors (www.plantcell.org) is: Yuling Jiao (yljiao@genetics.ac.cn).
[OPEN]Articles can be viewed without a subscription.
www.plantcell.org/cgi/doi/10.1105/tpc.16.00579

In addition to the SAM formed during embryogenesis, AMs form in the axils of leaves and develop into buds to enable branching (McConnell and Barton, 1998; Wang et al., 2016). Iterative branching in perennial plants can lead to thousands of terminal branches and thus determines aerial plant architecture (Wang and Li, 2008). The AM has the same developmental potential as the SAM to maintain itself and to initiate new organs. Genetic studies in *Arabidopsis thaliana* and other species have shown that AM initiation is regulated by several transcription factors, such as LATERAL SUPPRESSOR (LAS), REGULATOR OF AXILLARY MERISTEMS (RAX), and REVOLUTA (REV) (Talbert et al., 1995; Greb et al., 2003; Müller et al., 2006). Genetic and molecular studies revealed direct and indirect interactions among these genes in a regulatory network (Raman et al., 2008; Tian et al., 2014). *WUS* is expressed in the AM as in the SAM, but how *WUS* expression is established during AM initiation remains enigmatic. The FM shares many similarities with the AM and has been suggested to be a specialized AM (Long and Barton, 2000). How *WUS* expression is established in the FM is also unknown. Our recent work showed that initiation of both the AM and the FM requires a cytokinin signaling pulse (Han et al., 2014; Wang et al., 2014b).

In this study, we report that cytokinin promotes *WUS* expression to establish stem cell niches de novo during AM initiation. We then show that type-B Arabidopsis response regulator proteins (ARRs), which mediate the transcriptional response to cytokinin (Argyros et al., 2008), bind to the *WUS* promoter to activate its expression. We also show that *WUS* activation requires permissive chromatin modifications. In summary, we have provided a model for a direct molecular link explaining how shoot stem cell niches are established.

RESULTS

WUS Expression Is Activated de Novo during AM Initiation

To determine when *WUS* expression is established during AM initiation, we monitored the dynamics of leaf axil *WUS* expression in plants grown under short-day conditions for 28 d. Using the *ProWUS:DsRed-N7* reporter line for *WUS* expression (Gordon et al., 2007), we found that *WUS* expression is activated de novo prior to AM initiation. We did not detect *DsRed* expression in young leaf axils. We observed that *DsRed* expression in cells of the subepidermal layer started in the axil protrusions of the thirteenth oldest leaf primordium (P_{13}) (Figure 1A) and increased in P_{14} and older leaf axils (Figure 1B), a time when AMs are morphologically detectable (Long and Barton, 2000; Greb et al., 2003). At this stage, *WUS* is expressed in a small group of cells below the second cell layer of the AM (Figures 1A and 1B), resembling *WUS* expression in the SAM (Mayer et al., 1998). Thus, similar to the de novo activation of *WUS* expression during FM initiation (Mayer et al., 1998), de novo activation of *WUS* expression also occurs during AM initiation.

It has long been known that *WUS* is required for SAM and FM function (Laux et al., 1996), but it remains unknown if *WUS* is required for AM integrity. Therefore, we analyzed bud development in the *wus-1* and *wus-101* mutants. The *wus* mutants have a bushy phenotype due to repetitive initiation of defective shoot meristems (Laux et al., 1996). We carefully analyzed these defective shoot meristems and found that they all originated from leaf axils and were defective AMs. Because of their defective SAM, *wus* plants have reduced apical dominance and enhanced (terminated) axillary bud outgrowth. On the other hand, both *wus-1* and *wus-101* plants have a dramatic axillary bud formation defect (Figures 1C to 1J). We followed anatomical changes at the leaf axils of wild-type and *wus* plants. In P_{14} to P_{16} stage wild-type leaf axils, cells with a denser staining content form morphologically distinguishable bumps, which mark the first morphological change associated with AM development (Figures 1D and 1H). In both *wus-1* and *wus-101* plants, dense staining cells and AM structure are lost in comparable stage leaf axils at a high frequency (Figures 1F and 1J). Consistently, there is a dramatic reduction of axillary buds in *wus-1* (Figure 1C), with 77% (87 out of 113) of leaf axils not supporting the formation of axillary buds (Figure 1F; Supplemental Figure 1B), 6% (7 out of 113) of leaf axils forming one or two leaf-like structures (Supplemental Figure 1C), and 17% (19 out of 113) of leaf axils forming terminated buds (with three or more leaves). The combination of reduced apical dominance and outgrowth of occasionally formed but terminated buds led to the observed bushy phenotype. Notably, the AM initiation defect of *wus-101* can be rescued by *ProWUS:WUS-GFP* (Figure 1K) (Daum et al., 2014). Nevertheless, the *wus-1* and *wus-101* plants also have severe SAM defects, making it difficult to exclude an indirect effect of the SAM on AM initiation.

The expression of the meristematic gene *SHOOT MERISTEMLESS* (*STM*) marks leaf axil AM progenitor cells (Grbić and Bleecker, 2000; Long and Barton, 2000; Greb et al., 2003; Shi et al., 2016). Examination of accumulation of the *STM* transcript in the *wus-1* mutant by RNA in situ hybridization revealed a leaf axil expression pattern that is similar to the pattern in L*er* wild-type plants (Supplemental Figure 2), suggesting that the maintenance of meristematic cells does not rely on *WUS*.

Furthermore, *WUS* overexpression induced ectopic AM initiation. We used an inducible *WUS* overexpression line, *pga6-1* (Zuo et al., 2002), in which β-estradiol induces constitutive *WUS* overexpression, and a hormone-free leaf culture system (Wang et al., 2014b; Shi et al., 2016), in which we can quantify and live-image AM initiation. In isolated *pga6-1* leaves in culture, we found that β-estradiol induction can lead to the formation of additional AMs in the leaf axil (Supplemental Figures 3A and 3B). Ectopic *WUS* expression also leads to ectopic AM initiation in cotyledon axils, a phenotype indicating that AM initiation was enhanced (Wang et al., 2014a). Whereas wild-type Arabidopsis cotyledons lack axillary buds, we found that axillary buds could form in over 50% ($n > 10$) of cotyledon axils after *WUS* induction (Supplemental Figure 3C). To confirm that the ectopic AM initiation phenotype was due to *WUS* overexpression, but not potential second-site mutations, we generated an independent dexamethasone-inducible *WUS* overexpression line, *ProUBQ10:WUS-GR*. In *ProUBQ10:WUS-GR* leaf axils, we similarly observed ectopic AM formation after *WUS* induction (Supplemental Figure 3D). Additionally, a constitutive *WUS* overexpression line *sef*, which was isolated as an activation tagging mutant (Xu et al., 2005), showed multiple buds or branches per leaf axil (Supplemental Figures 3E

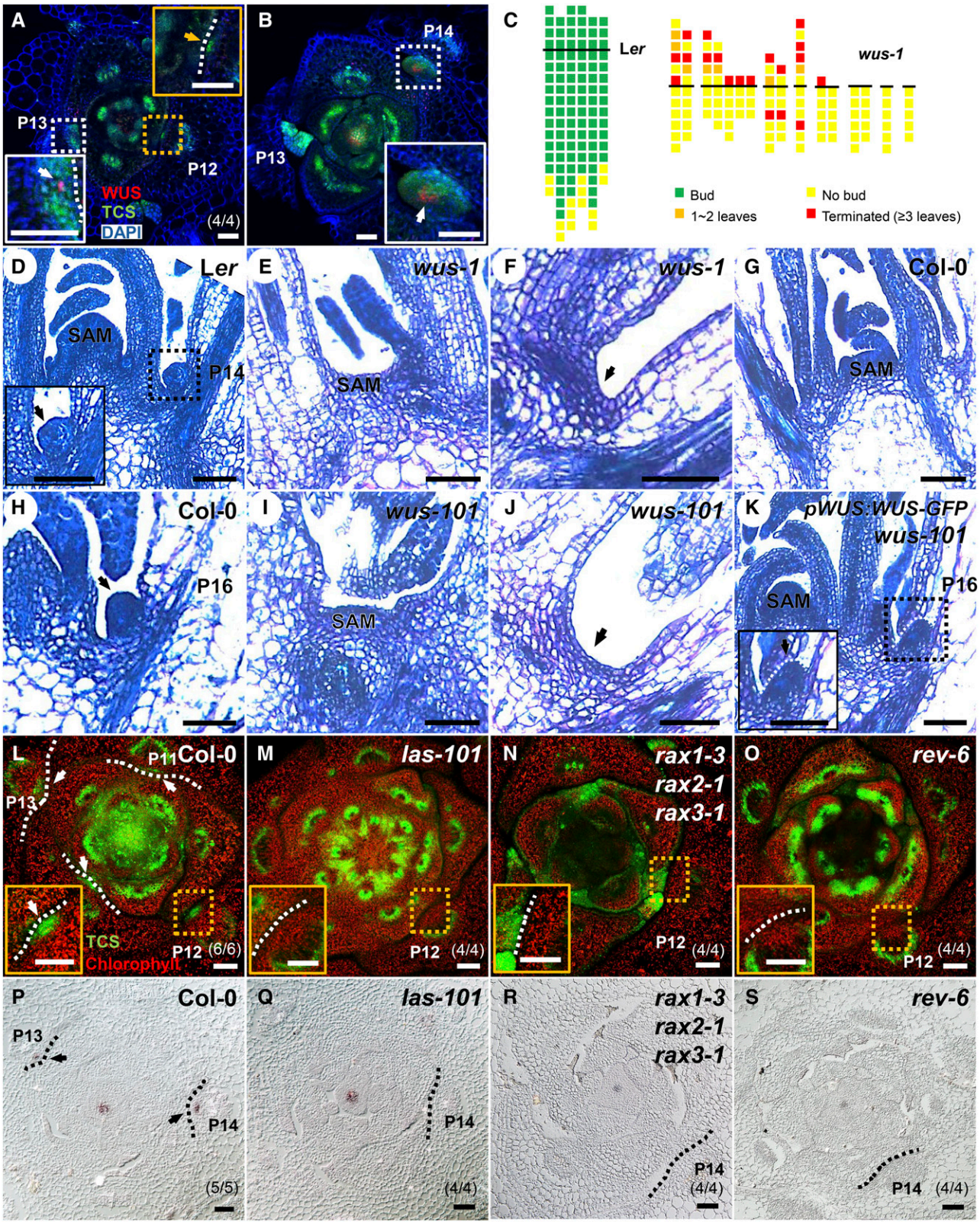

Figure 1. Cytokinin Signaling Precedes and Overlaps with *WUS* Expression prior to AM Initiation.

(A) and **(B)** Serial transverse sections through a wild-type vegetative shoot apex showing expression of *ProTCS:GFP-ER* (green) and *ProWUS:DsRed-N7* (red) in leaf axils. The orange arrow indicates GFP in the leaf axil, and white arrows indicate overlapping leaf axil GFP and DsRed signals. Sections are ordered from apical **(A)** to basal **(B)** parts from the same plant.

and 3F). Taken together, these findings indicated that *WUS* expression promoted AM initiation (Figure 1C).

Leaf Axil Cytokinin Signaling Precedes de Novo *WUS* Activation

Our recent work shows that a cytokinin signaling pulse occurs prior to AM initiation (Han et al., 2014; Wang et al., 2014b). We also used a cytokinin analog and a cytokinin antagonist to test whether AM initiation required cytokinin signaling. Treatment with the cytokinin analog 6-benzylaminopurine (BAP) caused production of multiple axillary buds (Supplemental Figures 4A to 4C). Treatment of detached leaf axils with the phenylquinazoline compound S-4893, a noncompetitive cytokinin antagonist that targets cytokinin receptors (Arata et al., 2010), severely compromised axillary bud formation (Supplemental Figure 4D).

To determine the dynamics of local cytokinin signaling and *WUS* expression in a developmental context, we examined the timing and location of expression of *ProTCS:GFP-ER* (Müller and Sheen, 2008), a cytokinin signaling reporter, in combination with *ProWUS:DsRed-N7*. Image analysis indicated that the leaf axil cytokinin signaling pulse emerged earlier than, and overlapped with, *WUS* expression during AM initiation (Figures 1A and 1B). Note that TCS signals in the leaf axil were substantially stronger than that in the SAM (Supplemental Figure 5) (Wang et al., 2014b), implying that the AM and SAM require different levels of cytokinin signaling. Taken together, these results indicated that de novo *WUS* activation during AM initiation is associated with a prior cytokinin signaling pulse in the same cells.

We also analyzed whether perturbed leaf axil cytokinin signaling was associated with defective *WUS* activation. AM initiation is compromised in the *las*, *rax*, and *rev* mutants (Talbert et al., 1995; Greb et al., 2003; Müller et al., 2006). Expression of the meristematic cell marker *STM* is maintained in *las* and *rev* mutants (Greb et al., 2003; Shi et al., 2016), suggesting that at least partial AM progenitor cell specification occurs in these mutants. We found that the leaf axils of these mutants lack the cytokinin signaling pulse (Figures 1L to 1O; Supplemental Figure 6A). In addition, we could not detect *WUS* expression in the leaf axils of these mutants (Figures 1P to 1S; Supplemental Figure 6B). Thus, lack of leaf axil cytokinin signaling associated with leaf axil *WUS* activation. Because cytokinin treatment can rescue AM initiation defects in *rax* mutants (Wang et al., 2014b), we speculate that cytokinin signaling activates *WUS* expression to enable AM initiation.

Cytokinin Activates *WUS* Expression

To test whether cytokinin signaling can activate *WUS* expression, we treated shoot tissues with the cytokinin analog BAP at a concentration of 0.89 μM, which is within physiological levels (Corbesier et al., 2003). To enrich leaf axil tissues, we removed leaves and used the remaining shoot tissue for gene expression analysis by RT-PCR with a limited number of cycles (see Methods). We found that a 4-h BAP treatment rapidly activated *WUS* expression, even in the presence of the protein synthesis inhibitor cycloheximide (CHX) (Figure 2A), suggesting that activation of *WUS* does not require de novo protein synthesis. Similarly, BAP activation of *WUS* expression was also found in the inflorescence (Supplemental Figure 7) (Gordon et al., 2009; Chickarmane et al., 2012), even when we used a physiological concentration of BAP (see Methods for details).

By live-imaging the expression of the *ProWUS:DsRed-N7* reporter and a functional *ProWUS:WUS-GFP* reporter (Daum et al., 2014), we found that BAP activated ectopic *WUS* expression centers de novo and substantially enlarged the endogenous *WUS* expressing domain. We employed a hormone-free leaf culture system to live-image AM initiation (Wang et al., 2014b; Shi et al., 2016). In isolated P_{15+} stage leaves, a 24-h BAP treatment induced multiple de novo centers of *WUS* expression in the leaf axil, so that the leaf axils formed multiple meristems, in contrast to the single meristem formed in untreated leaves (Figures 2B and 2C; Supplemental Figures 4A to 4C). In the leaf axil center where *WUS* normally is expressed, we observed a substantial enlargement of the *WUS* expression domain (Figures 2D to 2F; Supplemental Figures 8A to 8C, 9A to 9C, and 10). The expression of *WUS* was maintained in the center of the leaf axil until a visible axillary bud formed (Figures 2D to 2F). These results showed that local cytokinin signaling induced *WUS* expression in leaf axils to promote AM initiation. Consistent with this, mutants defective in cytokinin synthesis, perception, or signaling show defects in AM initiation (Wang et al., 2014b; Müller et al., 2015).

Figure 1. (continued).

(C) Schematic diagram of axillary buds of L*er* and *wus-1* plants. The thick black horizontal line represents the border between the youngest rosette leaf and the oldest cauline leaf. For L*er*, each column represents a single plant, and each square within a column represents an individual leaf axil. For *wus-1*, each column represents a single main branch, and branches from a single plant are grouped together. The bottom row represents the oldest rosette leaf axils, with progressively younger leaves above. Green, presence of an axillary bud; yellow, absence of an axillary bud; orange, one or two leaves in place of an axillary bud; red, a terminated axillary bud (with three or more leaves) in any particular leaf axil.

(D) to **(K)** Longitudinal sections of vegetative shoot apices. Images show a protruding AM in the leaf axil of L*er* **(D)**, Col-0 **(H)**, and *ProWUS:WUS-GFP wus-101* **(K)**, but the lack of an AM in the leaf axil of *wus-1* **(F)** and *wus-101* **(J)**. Note the normal SAM in L*er* **(D)**, Col-0 **(G)**, and *ProWUS:WUS-GFP wus-101* **(K)** in contrast to flat shoot apices in *wus-1* **(E)** and *wus-101* **(I)**. Black arrows indicate leaf axils.

(L) to **(O)** Expression of *ProTCS:GFP-ER* (green) in leaf axils. Images show transverse sections through shoot apices of Col-0 **(L)**, *las-101* **(M)**, *rax1-3 rax2-1 rax3-1* **(N)**, and *rev-6* mutants **(O)**. White arrows indicate GFP in leaf axils.

(P) to **(S)** In situ hybridization of *WUS* in the shoot apex. Images show transverse sections from Col-0 **(P)**, *las-101* **(Q)**, *rax1-3 rax2-1 rax3-1* **(R)**, and *rev-6* mutants **(S)**. Black arrows indicate *WUS* signal in leaf axils.

Dotted boxes indicate the locations of the regions magnified in the insets. Dotted lines indicate the outlines of leaf axils. P_n indicates leaf primordium number, and (m/n) indicates m in *n* of biological repeats showing the displayed features. Bars = 50 μm.

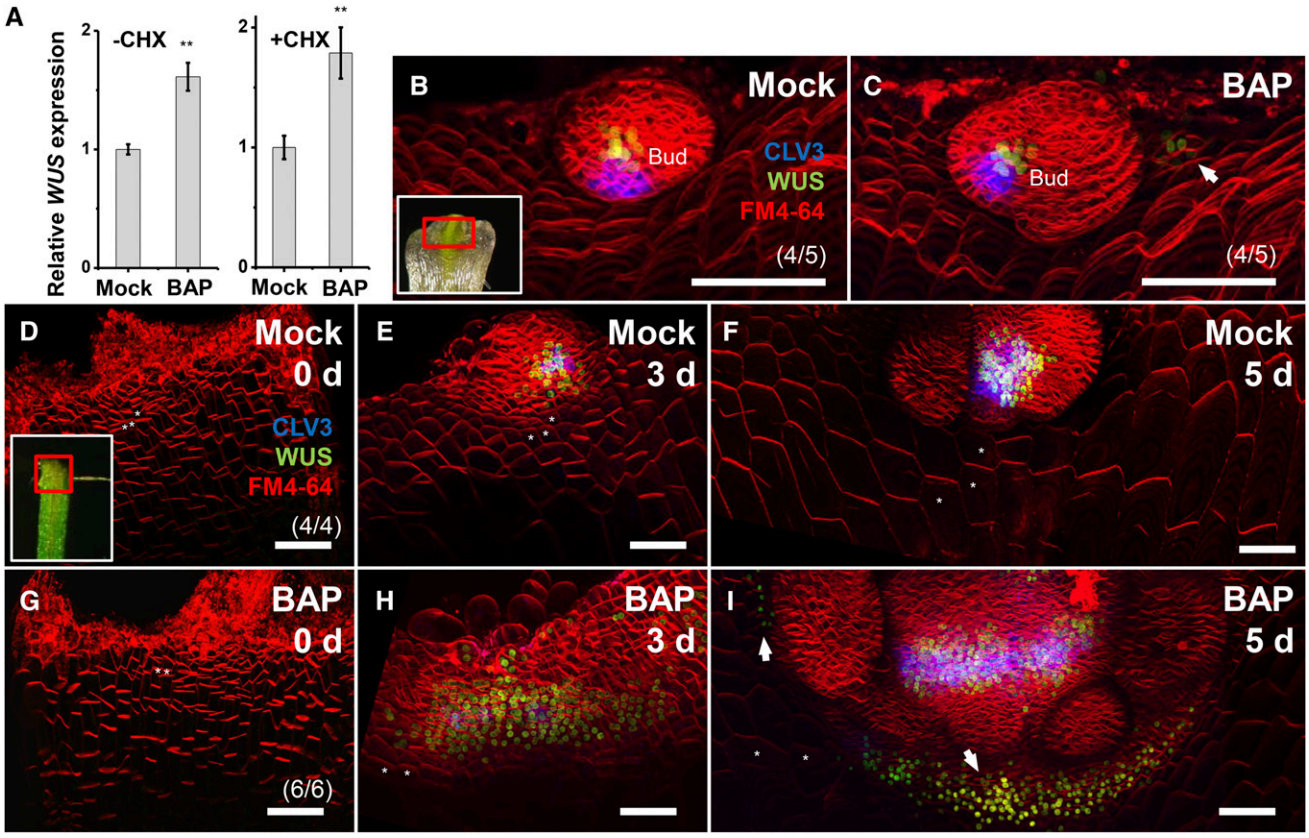

Figure 2. Induction of *WUS* Expression by Cytokinin Treatment.

(A) A 4-h 0.89 μM BAP treatment induced *WUS* expression in leaf-removed shoot apex tissues in both the absence and the presence of CHX. Error bars indicate the SD of three biological replicates, run in triplicate. **P < 0.01 (Student's *t* test).

(B) to **(I)** Time-lapse images of *WUS* expression in leaf axils. BAP treatment caused rapid induction of ectopic *ProWUS:DsRed-N7* in mature leaf axils **(C)** but delayed induction in immature leaf axils (**[G]** to **[I]**).

(B) and **(C)** A 24-h 0.89 μM BAP treatment **(C)**, but not mock treatment **(B)**, induced ectopic expression of *ProWUS:DsRed-N7* (green) in the leaf axil of an isolated P_{15} stage leaf (arrow).

(D) to **(I)** BAP treatment alters the *WUS* expression level, but not its timing. Time-lapse images showing expression of *ProWUS:DsRed-N7* (green) and *ProCLV3:GFP-ER* (blue) in isolated P_9 leaf axil centers after mock treatment (**[D]** to **[F]**) or 0.89 μM BAP treatment (**[G]** to **[I]**). BAP treatment caused the leaf axil center *WUS* expression domain to enlarge and activated ectopic *WUS* expression centers (arrows), but did not activate precocious *WUS* expression. The regions bordered by the red boxes in the insets in **(B)** and **(D)** roughly correspond to the imaged region. Asterisks in **(D)** to **(F)** and **(G)** to **(I)** label the same cells in corresponding time points. The cell membrane was labeled using FM4-64 (red). Bars = 50 μm.

In contrast to mature leaves (P_{15+}), ectopic cytokinin treatment of immature leaf axils or other tissues did not lead to precocious *WUS* activation. In isolated P_8 to P_{10} stage immature leaves, the expression of *ProWUS:DsRed-N7* was detectable in the center of the leaf axil at ~52 h in culture without the addition of BAP (Figures 2D to 2F; Supplemental Figures 8A to 8C and 9A to 9C). The expression of *ProCLV3:GFP-ER*, a *WUS* target, was detected 18 h later in the cells on top of the *WUS*-expressing cells (Supplemental Figures 9A to 9C). BAP treatment did not induce precocious *WUS* (and *CLV3*) expression (Supplemental Figure 9G). Nevertheless, BAP treatment induced additional de novo centers of *WUS* and *CLV3* expression accompanying the emergence of the central expression domain (Figure 2I). Also, the region of *ProWUS:DsRed-N7* and *ProCLV3:GFP-ER* expression in the central domain was substantially enlarged after BAP treatment (Figures 2G to 2I; Supplemental Figures 8D to 8F, 9D to 9F, and 10). In particular, BAP induced ectopic *WUS* expression in the epidermal cell layer (compared with Supplemental Figures 9B and 9E). The ectopic epidermal expression of *WUS* in the center of the leaf axil diminished when *CLV3* expression appeared (Supplemental Figure 9F). This may be explained by CLV3 inhibition of *WUS* expression (Gaillochet and Lohmann, 2015). The BAP treatment did not induce *WUS* expression in differentiated cells, such as leaf blade cells. Thus, our imaging results also suggested that the precise activation of *WUS* by cytokinins depended on the developmental stage and cell location (i.e., cell type).

WUS Expression Requires a Permissive Epigenetic Environment

Recent studies shows that the histone modification marker histone H3 lysine 27 trimethylation (H3K27me3), which is associated

with transcriptional repression, is highly enriched at the *WUS* locus in mature leaves, which have no *WUS* expression (Li et al., 2011; Liu et al., 2011). In addition, we found that histone H3 lysine 4 trimethylation (H3K4me3), a histone modification marker associated with transcriptional activation, was enriched at the *WUS* locus in inflorescences containing *WUS*-expressing cells but not in mature leaves lacking *WUS*-expressing cells (Supplemental Figure 11).

Stage-specific sensitivity of leaf axil cells to BAP treatment suggested that epigenetic modifications may change during leaf maturation. To test this hypothesis, we isolated the basal 2- to 3-mm leaf axil tissues from immature and mature leaves and analyzed histone modifications. To accommodate the limited sample amount, we used the ultralow input micrococcal nuclease-based native chromatin immunoprecipitation (ULI-NChIP) protocol (Brind'Amour et al., 2015). We found that the *WUS* genomic region showed higher levels of H3K27me3 and lower levels H3 acetylation in early stage (P_8 to P_{10}) leaf axils than in late stage (P_{15} to P_{17}) axils (Figures 3A to 3D). Histone acetylation increases the accessibility of DNA inside chromatin and promotes gene expression (Charron et al., 2009). Thus, the observed temporal histone modification changes correlate with activation of *WUS* expression in mature leaves, and stringent epigenetic modifications may prevent cytokinins from activating *WUS* expression in immature leaf axils and differentiated cells.

We next ectopically enhanced histone acetylation by applying the histone deacetylation inhibitor trichostatin A (TSA). TSA treatment, but not BAP treatment, increased histone H3 and H4 acetylation of the *WUS* genomic region (Supplemental Figure 12), which allows transcription. Whereas TSA treatment alone mildly increased the *WUS* expression level, which may be due to endogenous cytokinins, a 4-h cotreatment with BAP and TSA caused a 3.5-fold increase in *WUS* expression (Figure 3E). At the cellular level, we found that TSA enabled rapid de novo activation of *WUS* expression by BAP in differentiated leaf petiole cells (Figures 3F to 3I), explaining the dramatic increase of *WUS* levels by cotreatment with BAP and TSA.

We also used mutants that are defective in epigenetic repression of gene expression. The polycomb repressive complex (PRC) establishes the H3K27me3 mark and a repressive chromatin configuration (Schuettengruber et al., 2007). CURLY LEAF (CLF) is a PRC2 core component catalyzing H3K27me3, and RING1a and RING1b are PRC1 core components that bind to H3K27me3, inhibiting transcription (Goodrich et al., 1997; Argyros et al., 2008; Xu and Shen, 2008). We detected precocious *WUS* expression in young leaf axils of the *clf-29* mutant (Supplemental Figures 13A to 13B). In the *ring1a ring1b* mutant, we detected *WUS* expression in widely observed ectopic meristems (Supplemental Figure 13C). Furthermore, we found that the induction of *WUS* expression by BAP was significantly enhanced in these mutants (Figure 3J). Consistent with this, BAP induced more buds in isolated leaf axils of *clf-29* plants than in wild-type plants (Figure 3K). These results indicated that the PRC-mediated H3K27me3 repressed *WUS* in earlier leaf axil and differentiated tissues. Taken together, these results supported the idea that the induction of *WUS* required a permissive chromatin configuration.

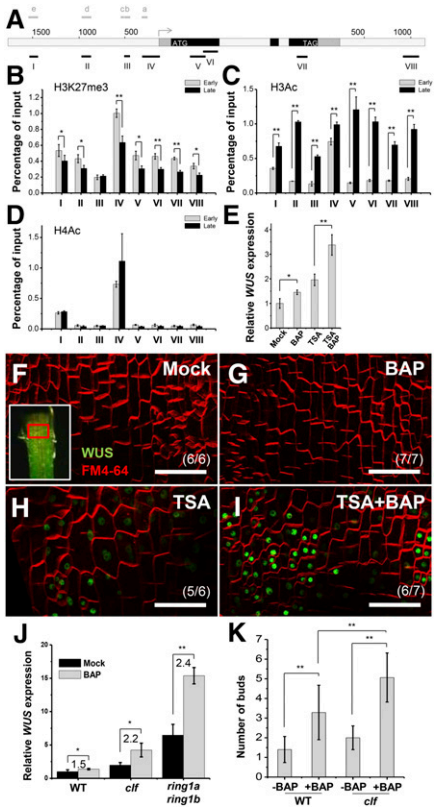

Figure 3. The Epigenetic Environment Affects Cytokinin Induction of *WUS* Expression.

(A) A diagram of the *WUS* genomic region with an arrow representing the transcription start site. Black, coding sequences; dark gray, untranslated regions; light gray, intron/intergenic regions; ATG and TAG, start and stop codons. Black bold lines with Roman numerals indicate fragments amplified by ChIP-qPCR. Gray bold lines with a to e indicate fragments showing in Figure 5A.

(B) to **(D)** The comparison of histone modifications in early and late stage of leaf axils. Images show ULI-NChIP with H3K27me3 **(B)**, and histone H3 **(C)** and H4 **(D)** acetylation of *WUS* genomic regions using early stage (P_8 to P_{10}) and late stage (P_{15} to P_{17}) leaf axil tissues. Error bars represent SD, which was calculated from three technical replicates. Two biological replicates gave similar results.

(E) Expression of *WUS* after a 4-h 0.89 μM BAP and/or 1 μM TSA treatment in shoot apex tissues. Leaves were removed before RNA isolation. Error bars indicate the SD of three biological replicates, run in triplicate.

(F) to **(I)** Expression of *ProWUS:DsRed-N7* (green) in P_9 leaf petiole cells. Images show *WUS* expression 15 h after mock **(F)**, 0.89 μM BAP **(G)**, 1 μM TSA **(H)**, or BAP and TSA **(I)** treatment. The regions bordered by the red box in the insets in **(F)** roughly correspond to the imaged region. Note that differentiated petiole cells were imaged. Bars = 50 μm.

(J) A 0.89 μM BAP treatment induced *WUS* expression in Col-0 wild-type, *clf-29*, and *ring1a ring1b* seedlings. Error bars indicate the SD of three biological replicates, run in triplicate.

(K) The number of buds in isolated leaf axils of Col-0 or *clf-29* mutants after a 2-week mock or BAP treatment. Error bars indicate the SD ($n \geq 10$). *P < 0.05 and **P < 0.01 (Student's *t* test).

ARR1 Activates *WUS* Expression

ARR1 is a typical type-B ARR mediating the transcriptional response to cytokinin (Argyros et al., 2008). We previously showed that the *arr1-4* loss-of-function mutant is defective in AM initiation (Wang et al., 2014b). Using a *ProARR1:GFP-N7* reporter line, we observed *ARR1* expression in the leaf axil, prior to and during AM initiation (Figure 4A). Furthermore, cell type-specific transcriptome data (Tian et al., 2014) show that many cytokinin signaling components, including other type-B ARRs, are expressed in the leaf axil (Supplemental Figure 14).

To test whether *ARR1* was required for *WUS* activation in the leaf axil, we analyzed *WUS* expression in the *arr1-4* mutant. We could not detect *WUS* expression in the leaf axil in *arr1-4* plants (Figures 4B to 4G). We next tested whether ARR1 can activate *WUS* expression during AM initiation using an inducible cytokinin-independent *ARR1ΔDDK-MYC* line, in which the N-terminal region encompassing the DDK domain was deleted (Guan et al., 2014). Phosphorylation of the Asp residue in the receiver domain activates the ability of the protein to promote the transcription of target genes. Because the DDK domain functions as a negative regulatory motif, its removal causes constitutive activation of transcription in the absence of cytokinin (Sakai et al., 2001). We found that activation of *ARR1ΔDDK-MYC* resulted in rapid induction of *WUS* expression both in shoot apex tissues and in the inflorescence within 8 h (Figure 4H; Supplemental Figure 15). Consistent with enhanced *WUS* expression, ectopic *ARR1ΔDDK-MYC* promoted AM initiation and bud outgrowth, resulting in a bushy phenotype. However, we did not observe ectopic meristem in leaves or on the stem, supporting the idea that *WUS* expression activation requires a permissive epigenetic environment.

We tested whether AM initiation defects in *arr1-4* can be rescued by restoring *WUS* expression using the inducible *WUS* overexpression line *pga6-1* (Zuo et al., 2002). In untreated *arr1-4 pga6-1* plants, very few of the first ~10 rosette leaves, which were formed during the first 2 weeks of vegetative development, develop axillary buds (Figure 4I). Starting at 15 d after germination, we treated shoot apexes of *arr1-4 pga6-1* plants with β-estradiol to induce *WUS* expression. We found that induction of *WUS* expression rescued the axillary bud formation defects (Figure 4I; Supplemental Figure 16). In addition, a substantial portion of the rosette leaves formed prior to treatment supported the formation of axillary buds after *WUS* induction (Figure 4I), suggesting that mature leaf axil cells of *arr1-4* plants are competent to respond to WUS activity. On the other hand, we did not observe precocious axillary bud formation after β-estradiol induction of *WUS* expression, suggesting that *WUS* expression is not sufficient for AM initiation. Taken together, these results indicated that ARR1 regulated AM initiation through activating *WUS* expression in the leaf axil. Because ARR10, 11, and 12 function redundantly with ARR1 in promoting AM initiation (Wang et al., 2014b), these related type-B ARRs may also promote *WUS* expression.

Type-B ARRs Bind to the *WUS* Promoter to Activate Its Expression

Because BAP induction of *WUS* did not require de novo protein synthesis (Figure 2A), we speculated that ARR1 and related type-B ARRs could bind directly to the *WUS* promoter region. Based on sequence conservation and the existence of the putative ARR1 binding site GAT(T/C) (Figures 5A and 5B; Supplemental Figure 17) (Sakai et al., 2000), we selected five regions of the *WUS* locus (a–e) for analysis.

Chromatin immunoprecipitation (ChIP) assays using either shoot tissues with leaves removed or inflorescence tissues showed that ARR1ΔDDK-MYC strongly associated with regions b, c, and d of the *WUS* promoter region (Figure 5C). To test whether ARR1 can directly bind to these regions, we performed an independent electrophoretic mobility shift assay (EMSA) and confirmed that the DNA binding domain of ARR1 bound to regions b, c, and d (Figure 5D; Supplemental Figure 18). Region c showed a lower affinity for the ARR1 protein than did regions b and d.

We also examined type-B ARR activation of *WUS* expression using a transient transfection assay, chosen because transiently expressed reporter constructs would lack epigenetic modifications that might interfere with ARR binding. Consistent with our ChIP and EMSA results, a transient transfection assay in protoplasts demonstrated that ARR1 activated the *WUS* promoter (Figure 5E; Supplemental Figures 19A and 19C). Regions b, c, and d are redundantly required for ARR1 activation (Figure 5F; Supplemental Figures 19B and 19D). Several other related type-B ARRs (Argyros et al., 2008) are expressed in the leaf axil (Supplemental Figure 14), and their mutations can enhance AM initiation defects in *arr1* mutants (Wang et al., 2014b). We then tested whether ARR2, 10, 11, and 12 could also directly activate *WUS* expression in protoplasts. Our results indicated that all of these type-B ARRs activated *WUS* expression, although to different extents (Figure 5G; Supplemental Figure 19E). This is consistent with their redundant roles in promoting AM initiation. Taken together, these results indicated that ARR1 and other related type-B ARRs can bind to the promoter of *WUS* to activate its expression.

DISCUSSION

WUS Expression Is Activated de Novo by Cytokinin Signaling during AM Initiation

Tremendous interest has focused on understanding how stem cells are specified in both animals and plants. Stem cell niches provide a microenvironment for stem cell fate determination and the establishment of stem cell niches is central to stem cell biology. In Arabidopsis, the expression of *WUS* defines shoot stem cell niches (Mayer et al., 1998), as shown by overexpression analyses (Zuo et al., 2002; Xu et al., 2005). Thus, understanding how *WUS* expression is regulated both spatially and temporally provides key information on stem cell niche specification. Several types of shoot meristems can form in plants. The SAM is established during embryonic development and AMs initiate post embryonically from the axils of leaves. Cells in AMs and the SAM have similar potential for indeterminate growth. After the floral transition, determinate FMs form and initiate a limited number of floral organs. Adventitious shoot meristems may also form, especially in tissue culture conditions. To understand how each type of shoot meristem is established, it is important to understand the

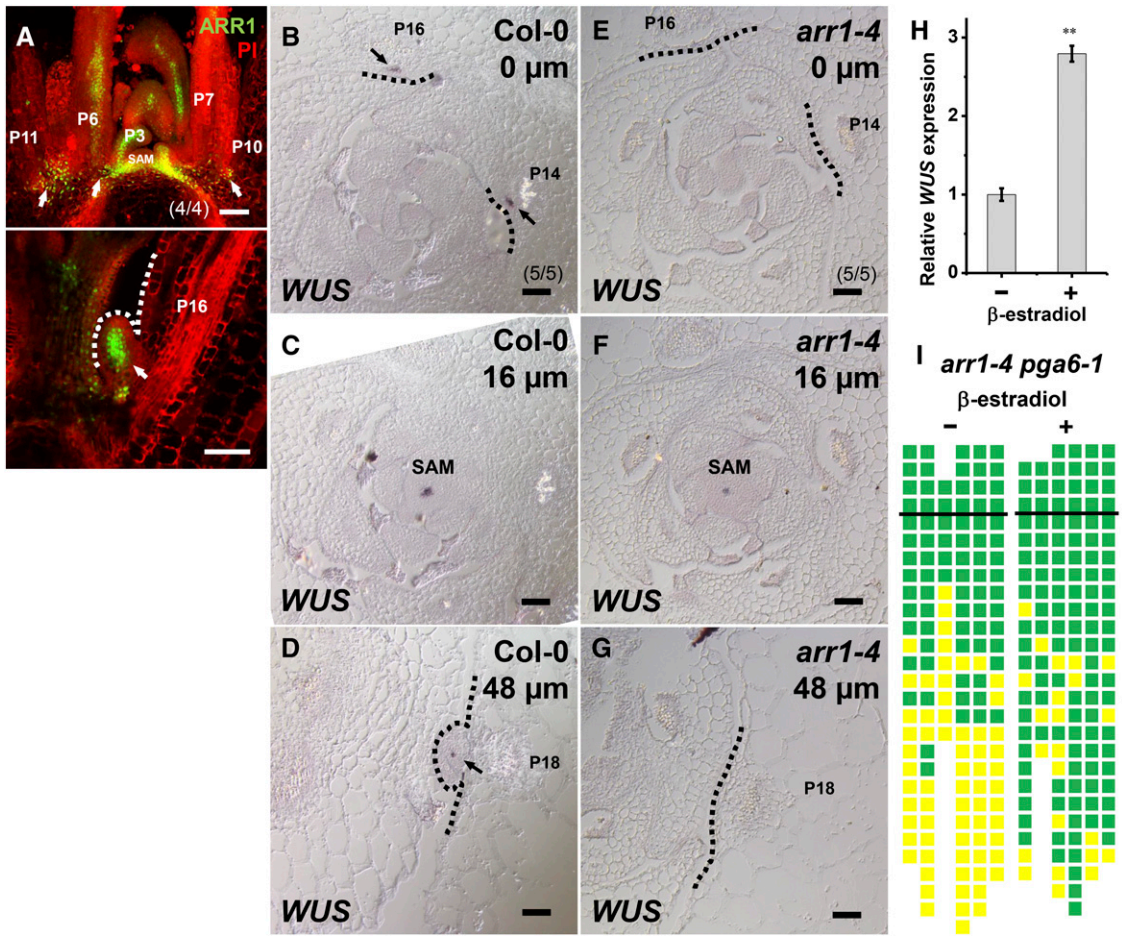

Figure 4. Activation of *WUS* Expression by ARR1 Is Required for AM Initiation.

(A) Expression of *ProARR1:GFP-N7* in the leaf axil. Images show longitudinal sections through a vegetative shoot apex demonstrating expression of *ProARR1:GFP-N7* (green) in the leaf axil prior to (upper panel) and during (lower panel) AM initiation. Arrows indicate GFP in leaf axils. The dotted line indicates the outline of the bulged meristem. PI, propidium iodide.

(B) to **(G)** In situ hybridization of *WUS*. Images show serial transverse sections of vegetative shoot apexes in Col-0 (**[B]** to **[D]**) and the *arr1-4* mutant (**[E]** to **[G]**). Arrows indicate *WUS* signal in leaf axils, and dotted lines indicate the outlines of leaf axils. Sections are ordered from apical (**[B]** and **[E]**) to basal (**[D]** and **[G]**). The approximate distance from the summit of the SAM to section is given in the upper right-hand corner of each image. Note that **(D)** and **(G)** are from regions more distant from the center of the same plants shown in **(B)** and **(C)**, and **(E)** and **(F)**. Bars in **(A)** to **(G)** = 50 μm.

(H) Expression of *WUS* after 8-h mock treatment or induction of *ARR1ΔDDK* in leaf-removed shoot tissues. Error bars indicate the SD of three biological replicates, run in triplicate. **$P < 0.01$ (Student's *t* test).

(I) Schematic diagram of axillary buds of *arr1-4 pga6-1* mutants with or without β-estradiol induction to activate *WUS* overexpression. See the legend to Figure 1C for a description of symbols. Green indicates the presence of an axillary bud, and yellow indicates the absence of an axillary bud. Plants were grown under short-day conditions for 15 d without treatment; leaf axil regions were treated with 10 μM β-estradiol every other day for another 15 d and then shifted to long-day conditions without treatment until axillary buds were counted. The vertical line indicates leaves initiated during β-estradiol treatment.

mechanism of activation of *WUS* expression during shoot meristem initiation.

In this study, we focused on the de novo activation of *WUS* expression during AM initiation. We previously showed that cytokinin promotes AM initiation (Han et al., 2014; Wang et al., 2014b). During AM initiation, the meristematic gene *STM* is highly expressed in the leaf axil (Grbić and Bleecker, 2000; Long and Barton, 2000; Greb et al., 2003; Shi et al., 2016). The leaf axil cytokinin signaling pulse may result from increased *STM* expression because STM can promote cytokinin biosynthesis (Jasinski et al., 2005; Yanai et al., 2005). In this study, we show that leaf axil cytokinin signaling directly increases the expression of *WUS*, which defines stem cell niches and completes AM initiation (Figure 6). The expression of cytokinin signaling pathway genes in the leaf axil (Figure 4A; Supplemental Figure 14), together with the STM-promoted cytokinin biosynthesis in the leaf axil, leads to the observed leaf axil-specific cytokinin signaling pulse and, more importantly, to de novo activation of *WUS* expression in the leaf axil (Figure 1). This activation is mediated by direct binding of ARR1 and related type-B ARRs, to the *WUS* promoter region

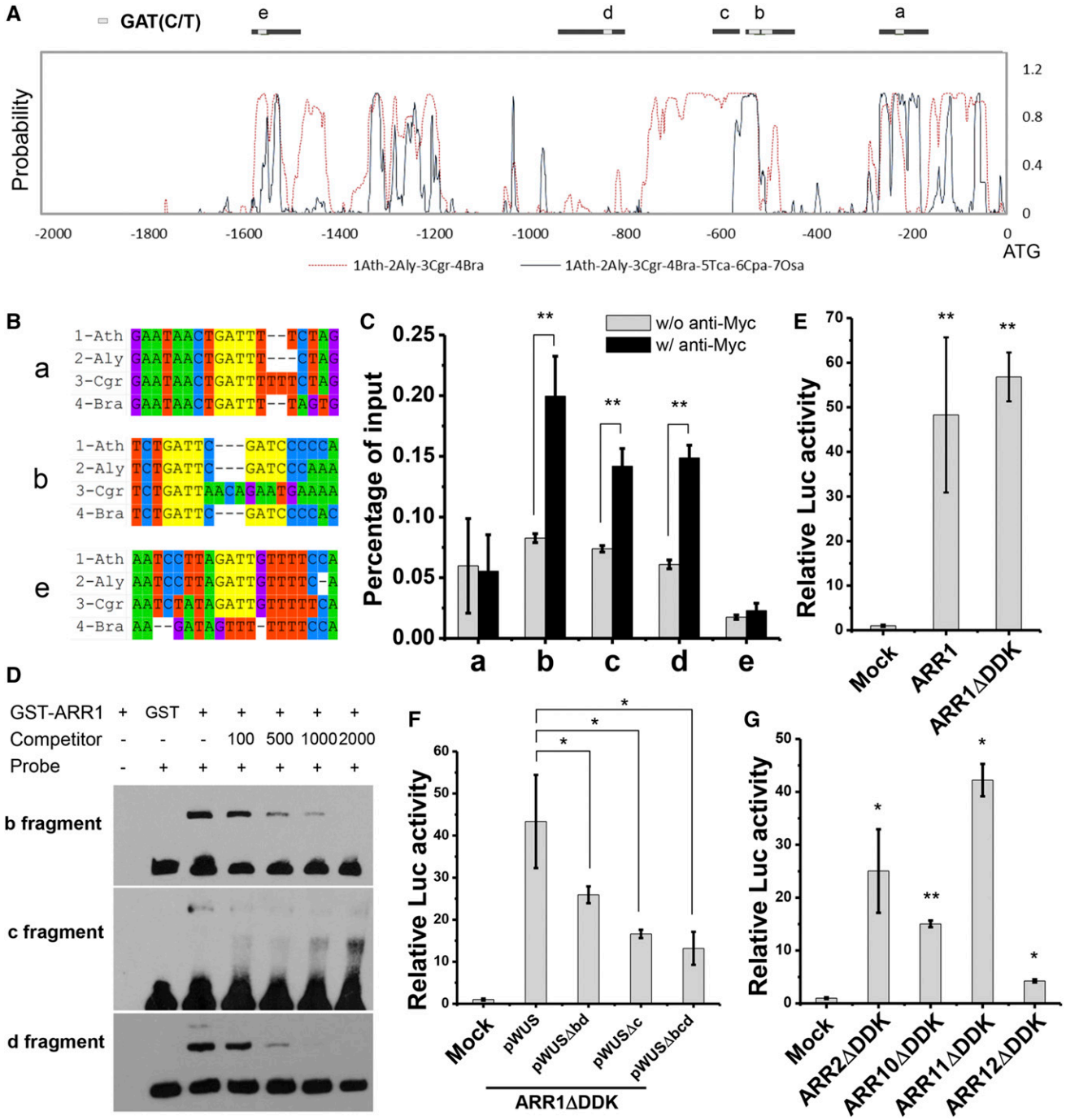

Figure 5. Direct Interaction of ARR1 with the *WUS* Promoter Region.

(A) and **(B)** Phylogenetic footprinting analysis of the *WUS* genomic region. Black bold lines with a to e indicate fragments amplified by ChIP-qPCR, and white boxes represent the GAT(T/C) in **(A)**, with adjacent sequences shown in **(B)**. Green, adenine; red, thymine; blue, cytosine; purple, guanine; yellow, conserved GAT(T/C) domain highlight.

(C) ChIP of ARR1ΔDDK-MYC protein with *WUS* chromatin regions. Shoot tissues (with leaves removed) were used.

(D) EMSA of ARRM-GST with the *WUS* genomic regions. ARRM indicates the DNA binding domain of ARR1.

(E) to **(G)** Ratio of firefly luciferase (Luc) to *Renilla* luciferase (Ren) activity in Arabidopsis protoplasts cotransformed with different reporter and effector construct combinations. Error bars in **(C)** to **(G)** indicate the SD of three biological replicates run in triplicate. *P < 0.05 and **P < 0.01 (Student's *t* test).

(Figure 5). The same regulatory principle likely functions during FM initiation (Supplemental Figures 7 and 15). In fact, floral bud development is also compromised in mutants defective in cytokinin synthesis, perception, or signaling, with phenotypes including defective floral bud initiation, fewer flowers, and early termination of inflorescences (Higuchi et al., 2004; Nishimura et al., 2004; Argyros et al., 2008; Tokunaga et al., 2012). The same regulatory circuits may also contribute to the de novo activation of *WUS* expression during embryonic SAM and adventitious shoot meristem formation. Recent studies have proposed that SAM maintenance requires cytokinin signaling (Gordon et al., 2009; Chickarmane et al., 2012). Therefore, the same regulatory principle may function during the maintenance of *WUS* expression. However, as shown by the *ProTCS:GFP* reporter, the SAM has much weaker cytokinin signaling than the leaf axil (Supplemental Figure 5), resulting from a lower cytokinin concentration and/or a weaker cytokinin response. This suggests that type-B ARR-based transcriptional activation may be insufficient to maintain *WUS* expression. Whether other regulatory mechanisms exist for maintenance of *WUS* expression in established shoot meristems remains to be answered.

WUS Is Required for AM Initiation and Integrity

In *wus* mutants, axillary buds are either absent or replaced by leaf-like structures that obviously lack indeterminate growth (Figures 1C to 1K; Supplemental Figure 1). A substantial portion (77%) of leaf axils are empty in *wus-1*, and most leaf axils lack discernible shoot meristem structure in *wus* mutants (Figures 1D to 1K), indicating that *WUS* is required for AM initiation. Although the *wus-1* and *wus-101* alleles we used are strong alleles with severe SAM defects, leaf patterning was mostly unaffected (Laux et al., 1996). Nevertheless, it is possible that the general effect of *WUS* on SAM function has an indirect role on AM initiation in the leaf axil. Recent studies also showed that formation of functional tiller buds in rice (*Oryza sativa*) requires the rice ortholog of *WUS* (Lu et al., 2015; Tanaka et al., 2015). In Arabidopsis *wus* mutants, leaf-like structures or even-terminal branches can still form in a portion of leaf axils (23% in *wus-1*; Figure 1C). Thus, additional regulators redundantly promote stem cell activities. Nevertheless, yet unknown stem cell activators are insufficient to maintain stem cell homeostasis and indeterminacy (Figure 1C).

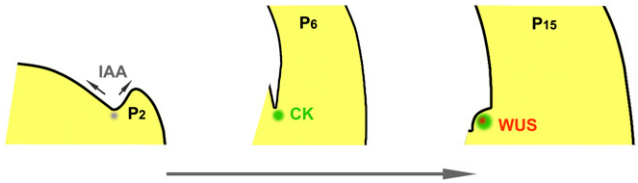

Figure 6. A Developmental Framework of AM Initiation.

In the leaf axil region, an auxin minimum (gray) at the early stage and a subsequent cytokinin signaling pulse (green) are required for AM initiation (Wang et al., 2014b). Later, cytokinin signaling de novo induces *WUS* expression (red) to activate the stem cell niche and complete AM initiation. IAA, indole acetic acid; CK, cytokinin.

It is plausible that *WUS* is required for stem cell initiation to promote AM initiation. Alternatively, defective stem cell homeostasis alone could explain the lack of AM in *wus* mutants. Recent work on embryonic shoot stem cell initiation indicated that *WUS* is dispensable for stem cell initiation and that several members of the *WUSCHEL-RELATED HOMEOBOX* gene family redundantly function in this process in embryos (Zhang et al., 2017). It remains to be tested whether *WUS* is required for stem cell initiation in the AM, in addition to its role in stem cell homeostasis.

STM is also necessary for AM initiation (Shi et al., 2016), and the expression of *STM* is maintained in the leaf axil in *wus-1* (Supplemental Figure 2). In contrast to the de novo activation of *WUS*, *STM* expression is maintained in the leaf axil (Grbić and Bleecker, 2000; Long and Barton, 2000; Greb et al., 2003; Shi et al., 2016). In fact, the expression patterns of *WUS* and *STM* are very different between AM initiation and embryogenesis. During embryogenesis, the onset of *WUS* expression at the 16-cell stage is much earlier than *STM* initiation at the late globular stage, when the embryo consists of ~100 cells (Lenhard and Laux, 1999). The continuous *STM* expression during AM initiation is consistent with the STM functions in shielding meristematic cells from differentiation, allowing later stem cell initiation (Shi et al., 2016). Nevertheless, STM may also provide rudimentary stem cell initiation activity in the absence of *WUS* (Brand et al., 2002).

Type-B ARRs Bind to the *WUS* Genomic Region

In addition to conducting genetic analysis, we provided multiple lines of evidence to support direct binding of ARR1 and related type-B ARRs, to the *WUS* promoter. ChIP, EMSA, and protoplast transactivation assays all demonstrated ARR binding to three discrete regions (b, c, and d) of the *WUS* promoter (Figure 5). Whereas regions b and d contain the canonical ARR1 binding core motif GAT(T/C) (Sakai et al., 2000), region c lacks this motif. EMSA showed weaker binding of ARR1 to region c compared with regions b and d (Figure 5D), implying an alternative DNA binding mechanism. Promoter deletion analysis indicated that these three regions are redundantly required for ARR activation of *WUS* expression (Figure 5F). The *wus-6* hypomorphic allele provides additional support for the importance of type-B ARR binding sites. In *wus-6*, a 7-kb T-DNA insertion separates the type-B ARR binding sites from the *WUS* open reading frame. The T-DNA insertion also caused a 95-bp deletion that partially overlaps with region b. The expression of *WUS* is substantially reduced in *wus-6* (Hamada et al., 2000), suggesting these evolutionarily conserved type-B ARR binding regions and/or additional upstream regions are important for *WUS* expression.

Notably, a *WUS* promoter lacking all three regions still showed activity, although the activity was much reduced (Figure 5F), indicating the existence of additional regulatory regions. One such candidate is a 57-bp region between regions c and d. A previous study showed that this region, when present in tandem and fused to a minimal CaMV 35S promoter, could drive *WUS* expression in the FM (Bäurle and Laux, 2005). Promoter deletion analysis also showed that flanking regions of the 57-bp core sequence, which covers regions c and d, were required for optimal promoter activity (Bäurle and Laux, 2005). This 57-bp region likely is sufficient for the maintenance of *WUS* expression, as this assay was done in

wild-type plants with functional FMs and endogenous *WUS* expression, but is insufficient for de novo activation of *WUS* expression. It again highlights that de novo activation of *WUS* expression prior to meristem initiation and maintenance of *WUS* expression in established meristems could use different molecular mechanisms.

Epigenetic Regulation Restricts *WUS* Expression

In addition to type-B ARR regulation, our work suggests that spatiotemporal epigenetic regulation refines *WUS* expression. Thus, hormones and epigenetic factors act in concert to govern formation of the lateral shoot stem cell niche. Although leaf axils have highly defined cytokinin signaling (Figure 1), additional cytokinin signaling centers exist in plants (Müller and Sheen, 2008). Type-B ARRs also have broad expression (Figure 4A; Supplemental Figure 14) (Mason et al., 2004). However, most cytokinin signaling centers do not activate *WUS* expression. Instead, in addition to cytokinin signaling, existing meristematic tissues are likely required to restrict spatiotemporal *WUS* expression. Our data indicated that increasing the chromatin accessibility by TSA treatment or in PRC mutants led to precocious and ectopic *WUS* expression and ectopic meristem formation following cytokinin treatment (Figures 3E to 3K; Supplemental Figure 13). Following TSA treatment of wild-type plants or PRC mutants, the onset of *WUS* expression in the leaf axil occurred earlier, and ectopic *WUS* appeared in differentiated cells (Figures 3F to 3I; Supplemental Figure 13) (Bratzel et al., 2010), resulting in ectopic meristems (Figure 3K; Supplemental Figure 13C). Epigenetic regulation is involved in the termination of *WUS* expression in the FM (Liu et al., 2011), and related mechanisms may suppress *WUS* expression in immature leave axil cells and in differentiated tissues. During leaf maturation, leaf axil cells divide (Wang et al., 2014b; Shi et al., 2016), and epigenetic modifications change (Figures 3A to 3D). This observation suggests a cell division-dependent induction, as was recently found in FM termination (Sun et al., 2014). Cell division may dilute inhibitory *cis*-acting marks and/or *trans*-acting factors so that the chromatin environment would be permissive for *WUS* expression. BAP does not affect prohibiting factors but TSA removes such factors (Figures 3E to 3I; Supplemental Figure 12). TSA treatment leads to different histone acetylation profiles of the *WUS* promoter than do endogenous regulators, indicating different site specificity. Nevertheless, TSA was efficient in conditioning BAP activation of *WUS*. The enrichment of H3K27me3, a marker of transcriptional repression, at the *WUS* locus in mature leaves and the enrichment of H3K4me3, a transcriptional activation marker, in inflorescences may be causal in the regulation of *WUS* expression (Supplemental Figure 11). Alternatively, these markers may simply reflect transcription status. The H3K4me3 binding protein REPRESSOR OF WUSCHEL1 may contribute to the epigenetic regulation of *WUS* in the leaf axil (Han et al., 2008; Zhang et al., 2015).

The activity of the AM determines plant architecture and crop yield (McSteen and Leyser, 2005; Wang and Li, 2008; Yang and Jiao, 2016). The finding that cytokinin activates *WUS* expression provides insight into how shoot stem cell niches are established and may ultimately facilitate the manipulation of plant architecture to enhance crop yield.

METHODS

Plant Materials and Treatment Conditions

Arabidopsis thaliana ecotypes Col-0, L*er*, and Ws were used as wild-type controls. Arabidopsis plants were grown under short-day conditions (8 h light and 16 h dark at 22°C) for 30 d and then under long-day conditions (16 h light and 8 h dark at 22°C) to induce flowering before axillary buds were counted. The transgenic lines *ProTCS:GFP*, *ARR1ΔDDK-MYC*, *ProWUS:WUS-GFP wus-101* (GK870H12), and *ProUBQ10:WUS-GR* are in the Col-0 background (Müller and Sheen, 2008; Daum et al., 2014; Guan et al., 2014), and *ProCLV3:GFP-ER ProWUS:DsRed-N7* is in the L*er* background (Reddy et al., 2004). The *wus-101*, *arr1-4*, *clf-29*, and *ring1a ring1b* mutants are in the Col-0 background (Goodrich et al., 1997; Argyros et al., 2008; Xu and Shen, 2008), the *wus-1* mutant is in the L*er* background (Laux et al., 1996), and the *pga6-1* and *sef* mutants are in the Ws background (Zuo et al., 2002; Xu et al., 2005). The *las*, *rax*, and *rev* mutants have been previously described (Talbert et al., 1995; Greb et al., 2003; Müller et al., 2006). For in vitro leaf culture, P_8 to P_{11} leaves were taken from plants grown on Murashige and Skoog medium in short-day conditions for 15 to 17 d. Detached leaves were cultured on Murashige and Skoog medium supplemented with 0.1 mg/L inositol acid and 0.5 mg/L folic acid under short-day conditions (Steeves et al., 1957; Wang et al., 2014b).

For chemical treatments, 0.89 μM BAP (Sigma-Aldrich), 30 μM S-4893 (3-[(6-chloro-4-phenylquinazolin-2-yl) amino] propan-1-ol; Vitas-M Laboratory) (Arata et al., 2010), 10 μM CHX (Sigma-Aldrich), and/or 1 μM TSA (Sigma-Aldrich) were used to treat 3-week-old short-day grown plants. For detached leaf culture, the solution was added to the leaf axil region. For seedlings and inflorescences, tissues were soaked in the solution. For inducible *WUS* expression, *pga6-1* and *arr1-4 pga6-1* plants were grown under short-day conditions for 15 d, treated with 10 μM β-estradiol every other day for 15 d, and then shifted to long-day conditions without β-estradiol treatment until axillary buds were counted (Zuo et al., 2002; Wang et al., 2014b). We used 6 to 16 plants for phenotypic analysis (Figures 1C, 3K, and 4I; Supplemental Figures 3 and 7).

In Situ Hybridization and Microscopy

In situ hybridization was performed as previously described (Wang et al., 2014b). The digoxigenin-labeled *WUS* probe contained nucleotides 382 to 1075 bp downstream of the start codon. Shoots were fixed and sectioned following previously described methods (Wang et al., 2014b). Images of sections and plants were taken by a Nikon SMZ1000 stereoscopic microscope or an Olympus BX60 microscope equipped with a Nikon DS-Ri1 camera. Scanning electron microscopy was performed using a Hitachi S-3000N variable pressure scanning electron microscope after standard tissue preparation (Wang et al., 2014b). For confocal microscopy, sample preparation was performed as previously described (Wang et al., 2014b). Images were taken with a Nikon A1 confocal microscope. Excitation and detection window setups for GFP, DsRed, 4′,6-diamidino-2-phenylindole, DsRed, GFP, FM4-64 (to label the cell membrane), and autofluorescence were previously described (Qi et al., 2014; Wang et al., 2014b). Ten to twenty replicates (in three batches) were analyzed.

RT-PCR and RT-qPCR

Total RNA was extracted from shoot tissues (with leaves removed), mature leaves, or inflorescences with the AxyPrep Multisource RNA MiniPrep kit (Corning). Arabidopsis shoot tissue is mainly composed of leaves, making leaf axil tissues low in abundance. As *WUS* expression is restricted to leaf axils, where axillary buds form, we removed leaves to enrich leaf axil tissues with *WUS* expression, so that its expression could be reliably detected. First-strand cDNA synthesis was performed using the TransScript One-Step gDNA Removal and cDNA Synthesis SuperMix (TransGen).

Quantitative RT-PCR was performed on a Bio-Rad CFX96 real-time detection system using the KAPA SYBR FAST qPCR kit (KAPA Biosystems) (Tian et al., 2014). *ACTIN2* was used as the reference gene to normalize the relative expression for quantitative RT-PCR analysis. RNAs from three batches of independently prepared plant materials (biological replicates with using different plants), each run in triplicate (technical replication), were analyzed. Mean and SD of biological replicates were used to present the data (Figures 2–5).

Phylogenetic Footprinting

The sequences of ~2000 bp upstream of the *WUS* start codon were aligned, and the degree of sequence divergence was quantified across for seven seed plant species (*Arabidopsis thaliana*, *Arabidopsis lyrata*, *Capsella grandiflora*, *Brassica rapa*, *Theobroma cacao*, *Carica papaya*, and *Oryza sativa*). All sequences were obtained from Phytozome 11.0 (https://phytozome.jgi.doe.gov/pz/portal.html). Sequence alignment (Supplemental File 1) was performed with ClustalX version 2.1 (Larkin et al., 2007) with gap opening = 10, gap extension = 0.2, delay divergent sequence = 30%, and turning off of negative matrix and Gonnet series for protein weight matrix. The phylogenetic tree for *WUS* (Supplemental File 1) was calculated with MEGA version 6.06 based on protein sequences (Tamura et al., 2013) using the neighbor-joining method (Saitou and Nei, 1987). Confidence intervals on phylogenies were inferred by the bootstrap method (Felsenstein, 1985). The evolutionary distances were computed using the Poisson correction method (Zuckerkandl and Pauling, 1965) and are in units of the number of amino acid substitutions per site. All positions containing gaps and missing data were eliminated. BigFoot, a Bayesian alignment and phylogenetic footprinting software, was then used to align genomic sequences and score the degree of conservation with default settings (Satija et al., 2009).

ChIP

ChIP experiments were performed according to published protocols (Han et al., 2014). Inflorescence or shoot tissues (with leaves removed) of ARR1ΔDDK-MYC plants were induced with 10 μM β-estradiol for 8 h. Samples of more than 800 mg of tissue were harvested and fixed with 1% (v/v) 4°C formaldehyde at 4°C (Han et al., 2014). Immunoprecipitations were performed with or without anti-MYC (ab9132; Abcam). The precipitated DNA was isolated, purified, and used as a template for quantitative RT-qPCR. For detection of histone modifications, seedlings, inflorescence, and leaves from Col-0 plants, and anti-H3K4m3 (ab8580; Abcam), anti-H3K27me3 (07-449; Millipore), anti-acetyl-Histone H3 (06-599; Millipore), and anti-acetyl-Histone H4 (06-598; Millipore) were used.

ULI-NChIP was performed according to published protocols with modifications (Brind'Amour et al., 2015). The basal 2 to 3 mm of leaf axil tissues from early stage (P_8 to P_{10}) or late stage (P_{15} to P_{17}) leaves were was isolated from 4- to 5-week-old wild-type Col-0 plants. Tissues from 30 to 40 leaf axils were used for each replicate. Tissues were fully ground with in 30 μL Galbraith buffer (45 mM $MgCl_2$, 30 mM sodium citrate, and 20 mM MES, pH 7.0) in a 1.5-mL tube. The pestle was washed with additional 20 μL Galbraith buffer into the same tube. Nuclei were spun down at 1000*g* for 10 min at 4°C. The supernatant was discarded, and the sediment was resuspended with 50 μL nuclear isolation buffer (NUC-101; Sigma-Aldrich). The subsequent chromatin preparation was based on micrococcal nuclease fragmentation at 37°C for 7 min. Chromatin was precleared with 10 μL of 1:1 protein A:protein G Dynabeads (Life Technologies) and then immunoprecipitated with 1 μg of antibody in antibody-bead complexes at 4°C overnight. Protein-DNA-bead complexes were washed twice with 400 μL low salt wash buffer (20 mM Tris-HCl, pH 8.0, 150 mM NaCl, 1% Triton X-100, and 0.1% SDS) and twice with high-salt wash buffer (20 mM Tris-HCl, pH 8.0, 500 mM NaCl, 1% Triton X-100, and 0.1% SDS). Protein-DNA complexes were eluted in 30 μL ChIP elution buffer (100 mM $NaHCO_3$ and 1% SDS). DNA was purified using phenol/chloroform and ethanol precipitation (Brind'Amour et al., 2015). The concentration of purified DNA was measured using the Qubit dsDNA HS Assay kit (1674653; Thermal Fisher) before the DNA was used as the template for PCR analysis.

EMSA

The DNA binding domain of ARR1 (ARRM; amino acids 236–299) fused with the GST tag was produced in a prokaryotic expression system as previously described (Tian et al., 2014). Biotin-labeled probes were amplified using 5′ biotin-labeled primers synthesized by Sangon Biotech, and corresponding competitor probes were amplified using primers of the same sequences without labeling. Binding reactions and competition experiments were performed as described (Tian et al., 2014).

Transient Expression in Protoplasts

Full-length coding sequences of *ARR1*, 460 bp downstream of the start codon of *ARR1* (*ARR1ΔDDK*), 433 bp downstream of the start codon of *ARR2* (*ARR2ΔDDK*), 400 bp downstream of the start codon of *ARR10* (*ARR10ΔDDK*), 382 bp downstream of the start codon of *ARR11* (*ARR11ΔDDK*), and 400 bp downstream of the start codon of *ARR12* (*ARR12ΔDDK*) were amplified from Arabidopsis cDNA by PCR and inserted between the *Kpn*I and *Bst*BI sites of the *ProUC19-p35S-FLAG-RBS* vector (Feng et al., 2012). To generate *ProWUS:Luc*, 1708 bp upstream of the start codon of *WUS* was amplified and inserted between the *Eco*RI and *Sac*I sites of the *ProFRK1:Luc* vector (Feng et al., 2012). *WUS* promoter deletions (*ProWUSΔ:Luc*) were obtained by inverse PCR using the *ProWUS:Luc* as the template. The conserved GAT(C/T) motifs were removed in *ProWUSΔbd* (Supplemental Figure 19B), and −617 to −599 bp were removed in *ProWUSΔc*.

Arabidopsis protoplasts were isolated from leaves of plants grown under short-day conditions for 5 to 6 weeks. The *ProUC19-Pro35S-ARRs-FLAG-RBS* vector was cotransformed with *ProWUS:Luc* (firefly luciferase) and *Pro35S:Ren* (*Renilla* luciferase) into protoplasts and incubated at room temperature overnight under weak light. The relative Luc activity (as relative Luc/Ren ratio) was detected with the dual-luciferase report assay system (Promega) and using a Promega GLOMAX 96 microplate luminometer. The efficiency of transient expression was quantified by western immunoblotting using anti-FLAG (A8592; Sigma-Aldrich).

Accession Numbers

Sequence data from this article can be found in the GenBank/EMBL database and/or the Arabidopsis Genome Initiative database under the following accession numbers: ACTIN2 (At3g18780), ARR1 (At3g16857), ARR2 (At4g16110), ARR10 (At4g31920), ARR11 (AT1G67710), ARR12 (At2g25180), CLF (At2g23380), CLV3 (At2g27250), LAS (AT1G55580), WUS/PGA6 (At2g17950), RAX1 (AT5G23000), RAX2 (AT2G36890), RAX3 (AT3G49690), REV (AT5G60690), RING1A (AT5G44280), RING1B (AT1G03770), STM (At1g62360), and UBQ10 (AT4G05320).

Supplemental Data

Supplemental Figure 1. Defective Axillary Bud Formation in the *wus-1* Mutant.

Supplemental Figure 2. In Situ Hybridization of *STM* in the *wus-1* Mutant.

Supplemental Figure 3. Bud Formation after *WUS* Overexpression.

Supplemental Figure 4. Regulation of Axillary Bud Initiation by Cytokinin.

Supplemental Figure 5. The Cytokinin Signaling Pulse Is Much Stronger in the Leaf Axil Than in the SAM.

Supplemental Figure 6. Lack of the Leaf Axil Cytokinin Signaling Pulse and *WUS* Expression in the *rax1-3* Mutant.

Supplemental Figure 7. BAP Induction of *WUS* Expression in the Inflorescence.

Supplemental Figure 8. Expression of *WUS-GFP* in Response to BAP Treatment in Immature Leaf Axils.

Supplemental Figure 9. Expression of *WUS* and *CLV3* in Response to BAP Treatment in the Center Region of Immature Leaves.

Supplemental Figure 10. BAP Treatment Enlarges the Expression Domain of *WUS* and *CLV3*.

Supplemental Figure 11. H3K4me3 Is Associated with the *WUS* Chromatin Region.

Supplemental Figure 12. Histone Acetylation of the *WUS* Genomic Region Increases Following TSA Treatment.

Supplemental Figure 13. In Situ Hybridization of *WUS* in *clf-29* and *ring1a ring1b* Mutants.

Supplemental Figure 14. Expression of Cytokinin Signaling and Biosynthesis Genes in the Leaf Axil.

Supplemental Figure 15. ARR1 Induction of *WUS* in the Inflorescence.

Supplemental Figure 16. Buds Formed by *WUS* Induction Are Identical to Normal Buds.

Supplemental Figure 17. Coding Sequence-Based Phylogenetic Tree of *WUS* from Seven Seed Plant Species.

Supplemental Figure 18. ARR1 No Longer Binds the Mutated Region b in an EMSA.

Supplemental Figure 19. Type-B ARRs Induce *WUS* Expression.

Supplemental Table 1. List of Primers.

Supplemental File 1. Text File of the Alignment Used for the Phylogenetic Analysis Shown in Supplemental Figure 17.

ACKNOWLEDGMENTS

We thank Ying Wang for critical reading of the manuscript, Kang Chong, Klaus Theres, Lin Xu, Yunyuan Xu, and Jianru Zuo for seeds, Jian-Min Zhou for the help with the transient expression assay, and Xian Sheng Zhang for exchanging unpublished results. This work was funded by National Natural Science Foundation of China (NSFC) Grant 31430010, by National Basic Research Program of China (973 Program) Grant 2014CB943500, by the National Program for Support of Top-Notch Young Professionals, and by the State Key Laboratory of Plant Genomics. C.T. is a member of the Youth Innovation Promotion Association of the Chinese Academy of Sciences (2017139).

AUTHOR CONTRIBUTIONS

Y.J. conceived the project. J.W., C.T., C.Z., B.S., and X.C. performed experiments and analyzed data. T.-Q.Z., Z.Z., and J.-W.W. contributed reagents. J.W. and Y.J. wrote the manuscript.

Received July 20, 2016; revised April 25, 2017; accepted June 1, 2017; published June 2, 2017.

REFERENCES

Arata, Y., Nagasawa-Iida, A., Uneme, H., Nakajima, H., Kakimoto, T., and Sato, R. (2010). The phenylquinazoline compound S-4893 is a non-competitive cytokinin antagonist that targets *Arabidopsis* cytokinin receptor CRE1 and promotes root growth in *Arabidopsis* and rice. Plant Cell Physiol. **51:** 2047–2059.

Argyros, R.D., Mathews, D.E., Chiang, Y.H., Palmer, C.M., Thibault, D.M., Etheridge, N., Argyros, D.A., Mason, M.G., Kieber, J.J., and Schaller, G.E. (2008). Type B response regulators of *Arabidopsis* play key roles in cytokinin signaling and plant development. Plant Cell **20:** 2102–2116.

Bäurle, I., and Laux, T. (2005). Regulation of *WUSCHEL* transcription in the stem cell niche of the *Arabidopsis* shoot meristem. Plant Cell **17:** 2271–2280.

Brand, U., Grünewald, M., Hobe, M., and Simon, R. (2002). Regulation of *CLV3* expression by two homeobox genes in *Arabidopsis.* Plant Physiol. **129:** 565–575.

Brand, U., Fletcher, J.C., Hobe, M., Meyerowitz, E.M., and Simon, R. (2000). Dependence of stem cell fate in *Arabidopsis* on a feedback loop regulated by CLV3 activity. Science **289:** 617–619.

Bratzel, F., López-Torrejón, G., Koch, M., Del Pozo, J.C., and Calonje, M. (2010). Keeping cell identity in *Arabidopsis* requires PRC1 RING-finger homologs that catalyze H2A monoubiquitination. Curr. Biol. **20:** 1853–1859.

Brind'Amour, J., Liu, S., Hudson, M., Chen, C., Karimi, M.M., and Lorincz, M.C. (2015). An ultra-low-input native ChIP-seq protocol for genome-wide profiling of rare cell populations. Nat. Commun. **6:** 6033.

Busch, W., et al. (2010). Transcriptional control of a plant stem cell niche. Dev. Cell **18:** 849–861.

Charron, J.B., He, H., Elling, A.A., and Deng, X.W. (2009). Dynamic landscapes of four histone modifications during deetiolation in *Arabidopsis.* Plant Cell **21:** 3732–3748.

Chickarmane, V.S., Gordon, S.P., Tarr, P.T., Heisler, M.G., and Meyerowitz, E.M. (2012). Cytokinin signaling as a positional cue for patterning the apical-basal axis of the growing *Arabidopsis* shoot meristem. Proc. Natl. Acad. Sci. USA **109:** 4002–4007.

Clark, S.E., Williams, R.W., and Meyerowitz, E.M. (1997). The *CLAVATA1* gene encodes a putative receptor kinase that controls shoot and floral meristem size in *Arabidopsis.* Cell **89:** 575–585.

Corbesier, L., Prinsen, E., Jacqmard, A., Lejeune, P., Van Onckelen, H., Périlleux, C., and Bernier, G. (2003). Cytokinin levels in leaves, leaf exudate and shoot apical meristem of *Arabidopsis thaliana* during floral transition. J. Exp. Bot. **54:** 2511–2517.

Daum, G., Medzihradszky, A., Suzaki, T., and Lohmann, J.U. (2014). A mechanistic framework for noncell autonomous stem cell induction in *Arabidopsis.* Proc. Natl. Acad. Sci. USA **111:** 14619–14624.

Felsenstein, J. (1985). Confidence limits on phylogenies: An approach using the Bootstrap. Evolution **39:** 783–791.

Feng, F., Yang, F., Rong, W., Wu, X., Zhang, J., Chen, S., He, C., and Zhou, J.M. (2012). A *Xanthomonas* uridine 5′-monophosphate transferase inhibits plant immune kinases. Nature **485:** 114–118.

Fletcher, J.C., Brand, U., Running, M.P., Simon, R., and Meyerowitz, E.M. (1999). Signaling of cell fate decisions by *CLAVATA3* in *Arabidopsis* shoot meristems. Science **283:** 1911–1914.

Gaillochet, C., and Lohmann, J.U. (2015). The never-ending story: from pluripotency to plant developmental plasticity. Development **142:** 2237–2249.

Goodrich, J., Puangsomlee, P., Martin, M., Long, D., Meyerowitz, E.M., and Coupland, G. (1997). A Polycomb-group gene regulates homeotic gene expression in *Arabidopsis.* Nature **386:** 44–51.

Gordon, S.P., Chickarmane, V.S., Ohno, C., and Meyerowitz, E.M. (2009). Multiple feedback loops through cytokinin signaling control stem cell number within the *Arabidopsis* shoot meristem. Proc. Natl. Acad. Sci. USA **106:** 16529–16534.

Gordon, S.P., Heisler, M.G., Reddy, G.V., Ohno, C., Das, P., and Meyerowitz, E.M. (2007). Pattern formation during de novo

assembly of the *Arabidopsis* shoot meristem. Development **134:** 3539–3548.

Grbić, V., and Bleecker, A.B. (2000). Axillary meristem development in *Arabidopsis thaliana.* Plant J. **21:** 215–223.

Greb, T., Clarenz, O., Schafer, E., Müller, D., Herrero, R., Schmitz, G., and Theres, K. (2003). Molecular analysis of the *LATERAL SUPPRESSOR* gene in *Arabidopsis* reveals a conserved control mechanism for axillary meristem formation. Genes Dev. **17:** 1175–1187.

Guan, C., Wang, X., Feng, J., Hong, S., Liang, Y., Ren, B., and Zuo, J. (2014). Cytokinin antagonizes abscisic acid-mediated inhibition of cotyledon greening by promoting the degradation of abscisic acid insensitive5 protein in *Arabidopsis.* Plant Physiol. **164:** 1515–1526.

Hamada, S., Onouchi, H., Tanaka, H., Kudo, M., Liu, Y.G., Shibata, D., MacHida, C., and Machida, Y. (2000). Mutations in the *WUSCHEL* gene of *Arabidopsis thaliana* result in the development of shoots without juvenile leaves. Plant J. **24:** 91–101.

Han, P., Li, Q., and Zhu, Y.X. (2008). Mutation of *Arabidopsis* BARD1 causes meristem defects by failing to confine *WUSCHEL* expression to the organizing center. Plant Cell **20:** 1482–1493.

Han, Y., Zhang, C., Yang, H., and Jiao, Y. (2014). Cytokinin pathway mediates *APETALA1* function in the establishment of determinate floral meristems in *Arabidopsis.* Proc. Natl. Acad. Sci. USA **111:** 6840–6845.

Higuchi, M., et al. (2004). In planta functions of the *Arabidopsis* cytokinin receptor family. Proc. Natl. Acad. Sci. USA **101:** 8821–8826.

Jasinski, S., Piazza, P., Craft, J., Hay, A., Woolley, L., Rieu, I., Phillips, A., Hedden, P., and Tsiantis, M. (2005). KNOX action in *Arabidopsis* is mediated by coordinate regulation of cytokinin and gibberellin activities. Curr. Biol. **15:** 1560–1565.

Larkin, M.A., et al. (2007). Clustal W and Clustal X version 2.0. Bioinformatics **23:** 2947–2948.

Laux, T., Mayer, K.F., Berger, J., and Jürgens, G. (1996). The *WUSCHEL* gene is required for shoot and floral meristem integrity in *Arabidopsis.* Development **122:** 87–96.

Leibfried, A., To, J.P., Busch, W., Stehling, S., Kehle, A., Demar, M., Kieber, J.J., and Lohmann, J.U. (2005). WUSCHEL controls meristem function by direct regulation of cytokinin-inducible response regulators. Nature **438:** 1172–1175.

Lenhard, M., and Laux, T. (1999). Shoot meristem formation and maintenance. Curr. Opin. Plant Biol. **2:** 44–50.

Lenhard, M., Bohnert, A., Jürgens, G., and Laux, T. (2001). Termination of stem cell maintenance in *Arabidopsis* floral meristems by interactions between WUSCHEL and AGAMOUS. Cell **105:** 805–814.

Li, W., Liu, H., Cheng, Z.J., Su, Y.H., Han, H.N., Zhang, Y., and Zhang, X.S. (2011). DNA methylation and histone modifications regulate de novo shoot regeneration in *Arabidopsis* by modulating *WUSCHEL* expression and auxin signaling. PLoS Genet. **7:** e1002243.

Liu, X., Kim, Y.J., Müller, R., Yumul, R.E., Liu, C., Pan, Y., Cao, X., Goodrich, J., and Chen, X. (2011). *AGAMOUS* terminates floral stem cell maintenance in *Arabidopsis* by directly repressing *WUSCHEL* through recruitment of Polycomb Group proteins. Plant Cell **23:** 3654–3670.

Lohmann, J.U., Hong, R.L., Hobe, M., Busch, M.A., Parcy, F., Simon, R., and Weigel, D. (2001). A molecular link between stem cell regulation and floral patterning in *Arabidopsis.* Cell **105:** 793–803.

Long, J., and Barton, M.K. (2000). Initiation of axillary and floral meristems in *Arabidopsis.* Dev. Biol. **218:** 341–353.

Lu, Z., Shao, G., Xiong, J., Jiao, Y., Wang, J., Liu, G., Meng, X., Liang, Y., Xiong, G., Wang, Y., and Li, J. (2015). *MONOCULM 3*, an ortholog of *WUSCHEL* in rice, is required for tiller bud formation. J. Genet. Genomics **42:** 71–78.

Müller, B., and Sheen, J. (2008). Cytokinin and auxin interaction in root stem-cell specification during early embryogenesis. Nature **453:** 1094–1097.

Müller, D., Schmitz, G., and Theres, K. (2006). *Blind* homologous R2R3 Myb genes control the pattern of lateral meristem initiation in *Arabidopsis.* Plant Cell **18:** 586–597.

Müller, D., Waldie, T., Miyawaki, K., To, J.P., Melnyk, C.W., Kieber, J.J., Kakimoto, T., and Leyser, O. (2015). Cytokinin is required for escape but not release from auxin mediated apical dominance. Plant J. **82:** 874–886.

Mason, M.G., Li, J., Mathews, D.E., Kieber, J.J., and Schaller, G.E. (2004). Type-B response regulators display overlapping expression patterns in Arabidopsis. Plant Physiol. **135:** 927–937.

Mayer, K.F., Schoof, H., Haecker, A., Lenhard, M., Jürgens, G., and Laux, T. (1998). Role of *WUSCHEL* in regulating stem cell fate in the *Arabidopsis* shoot meristem. Cell **95:** 805–815.

McConnell, J.R., and Barton, M.K. (1998). Leaf polarity and meristem formation in *Arabidopsis.* Development **125:** 2935–2942.

McSteen, P., and Leyser, O. (2005). Shoot branching. Annu. Rev. Plant Biol. **56:** 353–374.

Nishimura, C., Ohashi, Y., Sato, S., Kato, T., Tabata, S., and Ueguchi, C. (2004). Histidine kinase homologs that act as cytokinin receptors possess overlapping functions in the regulation of shoot and root growth in *Arabidopsis.* Plant Cell **16:** 1365–1377.

Ogawa, M., Shinohara, H., Sakagami, Y., and Matsubayashi, Y. (2008). *Arabidopsis* CLV3 peptide directly binds CLV1 ectodomain. Science **319:** 294.

Qi, J., Wang, Y., Yu, T., Cunha, A., Wu, B., Vernoux, T., Meyerowitz, E., and Jiao, Y. (2014). Auxin depletion from leaf primordia contributes to organ patterning. Proc. Natl. Acad. Sci. USA **111:** 18769–18774.

Raman, S., Greb, T., Peaucelle, A., Blein, T., Laufs, P., and Theres, K. (2008). Interplay of *miR164, CUP-SHAPED COTYLEDON* genes and *LATERAL SUPPRESSOR* controls axillary meristem formation in *Arabidopsis thaliana.* Plant J. **55:** 65–76.

Reddy, G.V., Heisler, M.G., Ehrhardt, D.W., and Meyerowitz, E.M. (2004). Real-time lineage analysis reveals oriented cell divisions associated with morphogenesis at the shoot apex of *Arabidopsis thaliana.* Development **131:** 4225–4237.

Saitou, N., and Nei, M. (1987). The neighbor-joining method: a new method for reconstructing phylogenetic trees. Mol. Biol. Evol. **4:** 406–425.

Sakai, H., Aoyama, T., and Oka, A. (2000). *Arabidopsis* ARR1 and ARR2 response regulators operate as transcriptional activators. Plant J. **24:** 703–711.

Sakai, H., Honma, T., Aoyama, T., Sato, S., Kato, T., Tabata, S., and Oka, A. (2001). ARR1, a transcription factor for genes immediately responsive to cytokinins. Science **294:** 1519–1521.

Satija, R., Novák, A., Miklós, I., Lyngsø, R., and Hein, J. (2009). BigFoot: Bayesian alignment and phylogenetic footprinting with MCMC. BMC Evol. Biol. **9:** 217.

Schoof, H., Lenhard, M., Haecker, A., Mayer, K.F., Jürgens, G., and Laux, T. (2000). The stem cell population of *Arabidopsis* shoot meristems in maintained by a regulatory loop between the *CLAVATA* and *WUSCHEL* genes. Cell **100:** 635–644.

Schuettengruber, B., Chourrout, D., Vervoort, M., Leblanc, B., and Cavalli, G. (2007). Genome regulation by polycomb and trithorax proteins. Cell **128:** 735–745.

Shi, B., et al. (2016). Two-step regulation of a meristematic cell population acting in shoot branching in *Arabidopsis.* PLoS Genet. **12:** e1006168.

Steeves, T.A., Gabriel, H.P., and Steeves, M.W. (1957). Growth in sterile culture of excised leaves of flowering plants. Science **126:** 350–351.

Sun, B., Looi, L.S., Guo, S., He, Z., Gan, E.S., Huang, J., Xu, Y., Wee, W.Y., and Ito, T. (2014). Timing mechanism dependent on cell division is invoked by Polycomb eviction in plant stem cells. Science **343:** 1248559.

Talbert, P.B., Adler, H.T., Parks, D.W., and Comai, L. (1995). The *REVOLUTA* gene is necessary for apical meristem development and for limiting cell divisions in the leaves and stems of *Arabidopsis thaliana.* Development **121:** 2723–2735.

Tamura, K., Stecher, G., Peterson, D., Filipski, A., and Kumar, S. (2013). MEGA6: Molecular Evolutionary Genetics Analysis version 6.0. Mol. Biol. Evol. **30:** 2725–2729.

Tanaka, W., Ohmori, Y., Ushijima, T., Matsusaka, H., Matsushita, T., Kumamaru, T., Kawano, S., and Hirano, H.Y. (2015). Axillary meristem formation in rice requires the *WUSCHEL* ortholog *TILLERS ABSENT1.* Plant Cell **27:** 1173–1184.

Tian, C., et al. (2014). An organ boundary-enriched gene regulatory network uncovers regulatory hierarchies underlying axillary meristem initiation. Mol. Syst. Biol. **10:** 755.

Tokunaga, H., Kojima, M., Kuroha, T., Ishida, T., Sugimoto, K., Kiba, T., and Sakakibara, H. (2012). *Arabidopsis lonely guy* (*LOG*) multiple mutants reveal a central role of the LOG-dependent pathway in cytokinin activation. Plant J. **69:** 355–365.

Wang, Q., Hasson, A., Rossmann, S., and Theres, K. (2016). *Divide et impera*: boundaries shape the plant body and initiate new meristems. New Phytol. **209:** 485–498.

Wang, Q., Kohlen, W., Rossmann, S., Vernoux, T., and Theres, K. (2014a). Auxin depletion from the leaf axil conditions competence for axillary meristem formation in *Arabidopsis* and tomato. Plant Cell **26:** 2068–2079.

Wang, Y., and Li, J. (2008). Molecular basis of plant architecture. Annu. Rev. Plant Biol. **59:** 253–279.

Wang, Y., Wang, J., Shi, B., Yu, T., Qi, J., Meyerowitz, E.M., and Jiao, Y. (2014b). The stem cell niche in leaf axils is established by auxin and cytokinin in *Arabidopsis.* Plant Cell **26:** 2055–2067.

Xu, L., and Shen, W.H. (2008). Polycomb silencing of *KNOX* genes confines shoot stem cell niches in *Arabidopsis.* Curr. Biol. **18:** 1966–1971.

Xu, Y.Y., Wang, X.M., Li, J., Li, J.H., Wu, J.S., Walker, J.C., Xu, Z.H., and Chong, K. (2005). Activation of the *WUS* gene induces ectopic initiation of floral meristems on mature stem surface in *Arabidopsis thaliana.* Plant Mol. Biol. **57:** 773–784.

Yadav, R.K., Perales, M., Gruel, J., Girke, T., Jönsson, H., and Reddy, G.V. (2011). WUSCHEL protein movement mediates stem cell homeostasis in the *Arabidopsis* shoot apex. Genes Dev. **25:** 2025–2030.

Yadav, R.K., Perales, M., Gruel, J., Ohno, C., Heisler, M., Girke, T., Jönsson, H., and Reddy, G.V. (2013). Plant stem cell maintenance involves direct transcriptional repression of differentiation program. Mol. Syst. Biol. **9:** 654.

Yanai, O., Shani, E., Dolezal, K., Tarkowski, P., Sablowski, R., Sandberg, G., Samach, A., and Ori, N. (2005). *Arabidopsis* KNOXI proteins activate cytokinin biosynthesis. Curr. Biol. **15:** 1566–1571.

Yang, M., and Jiao, Y. (2016). Regulation of axillary meristem initiation by transcription factors and plant hormones. Front. Plant Sci. **7:** 183.

Zhang, Y., Jiao, Y., Liu, Z., and Zhu, Y.X. (2015). ROW1 maintains quiescent centre identity by confining *WOX5* expression to specific cells. Nat. Commun. **6:** 6003.

Zhang, Z., Tucker, E., Hermann, M., and Laux, T. (2017). A molecular framework for the embryonic initiation of shoot meristem stem cells. Dev. Cell **40:** 264–277.e4.

Zhou, Y., Liu, X., Engstrom, E.M., Nimchuk, Z.L., Pruneda-Paz, J.L., Tarr, P.T., Yan, A., Kay, S.A., and Meyerowitz, E.M. (2015). Control of plant stem cell function by conserved interacting transcriptional regulators. Nature **517:** 377–380.

Zuckerkandl, E., and Pauling, L. (1965). Evolutionary divergence and convergence in proteins. In Evolving Genes and Proteins, V. Vogel and H.J. Bryson, eds (Academic Press), pp. 97–166.

Zuo, J., Niu, Q.W., Frugis, G., and Chua, N.H. (2002). The *WUSCHEL* gene promotes vegetative-to-embryonic transition in *Arabidopsis.* Plant J. **30:** 349–359.